- Technical Paper -

INFLUENCE OF TOP FLANGE TO SHEAR RESISTING MECHANISM OF REINFORCED CONCRETE T-BEAMS

Withit PANSUK [*1], Yasuhiko SATO [*2], Ryosuke TAKAHASHI [*3] and Tamon UEDA [*4]

ABSTRACT

In this paper, how the top flange area affects shear capacity of RC T-beam with shear reinforcement is discussed based on experimental and analytical observations. The turning point of the shear resisting mechanism from the truss analogy to the arch mechanism can be observed from the tested and FEM results. The influence of the horizontal crack on the shear mechanism is discussed.

Keywords: T-beams, top flange area, shear resisting mechanism, and 3D finite element method

1. INTRODUCTION

In the slab-beam-girder structure system, the beams are usually built monolithically with the slab. Hence, the portion of concrete slab, effectively connected together with beam, can be considered as the flange projecting from each side of beam. At the same time, the part of beam at the bottom of slab is working as the web of T-shaped beam or simply T-beams. As well known, in the current design code, shear strength of beam can be calculated based on the modified truss theory, in which effects of top flange area of T-beam cannot be considered. However the area of top flange may affects shear capacity when a beam would fail in shear compression mode. To predict the shear capacity of T-beam more precisely, the effect of the concrete top flange area on shear resisting mechanism must be clarified.

In order to study how concrete top flange work in a shear problem of T-beams, two RC beam specimens, rectangular and T-beams, were tested. Some general experimental and numerical results such as load-deformation curve, stirrup stress, failure mode, and crack pattern have already been reported in the earlier work [1]. Consequently, the objective of the present study is to demonstrate the both experimental and analytical results in the term of the shear resisting mechanism of T-beams. And, some verification of the mechanism has been done by the numerical technique.

2. TEST PROGRAMS

2.1 Outline of Program

Two reinforced concrete beams of rectangular and T-shape sections were tested. The rectangular beam had the size of 3800×150×350 mm (length×width×height) and effective depth of 300 mm. For T-shaped, the cross section was almost the same as rectangular beam; only concrete flange was attached in the top position of a whole long beam. The stirrups in the tested part had the spacing of 110 mm, while stirrups were placed heavier in the remaining parts of beam to ensure the shear failure within the tested span. The full details of their dimensions, arrangement of reinforcing steel and loading condition are shown in Fig.1.

*1 Graduate School of Engineering, Hokkaido University, JCI Member
*2 Research Associate, Dept. of Civil Engineering, Hokkaido University, Dr.E., JCI Member
*3 Research Engineer, Port and Airport Research Institute, Yokosuka, Dr.E., JCI Member
*4 Prof., Dept. of Civil Engineering, Hokkaido University, Dr.E., JCI Member

2.2 Materials

Both specimens had the same tension and compression reinforcement, four of D25 and two of D10 respectively. Shear reinforcement was D6 stirrup with closed-hoop shape. Fig.2 shows cross sections of specimens. Concrete cylinder strength (f_c') for each specimen was 35 MPa. The main reinforcement ratio and shear reinforcement ratio were 4% and 0.4%, respectively. The properties of steel used are given in Table 1.

2.3 Test Method and Measurement

The load was applied through a steel loading beam with the spherical bearing unit at the both load points. Steel plate 90 mm wide by 15 mm thick were used to distribute loads and support reactions. For both specimens, the load was applied in 10-kN increments until 180 kN and released until zero. And, the load was applied in the same increments up to failure. Strain gages were attached to measure strain in each stirrup at distances of 60, 130 and 220 mm above the centroid of the tension reinforcement for both specimens. Also, strain gages were attached to measure strains in main bars at distances of 350, 525, 700, 965 and 1500 mm from support for checking yielding of the bars and drawing the strain distribution on sections. In the experiment, two types of strain gages for concrete, inside concrete and on concrete surface, were installed into both specimens for measuring strains in *X* (parallel to main bars) direction. The measured sections are at the area near loading plate (at the location of stirrup No.1 in Fig.5) and the middle of shear span (at the location of stirrup No.5 in Fig.5). Locations of concrete strain gages at both sections are shown in Fig.3.

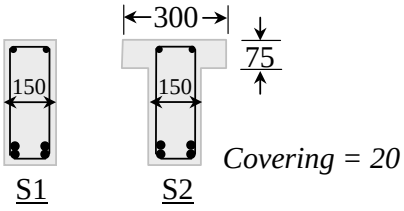

Fig.2 Cross sections (unit: mm)

3. OUTLINE OF ANALYSIS

In the present study, a three-dimensional nonlinear finite element program (CAMUI) developing at the Hybrid Structure Engineering Laboratory of Hokkaido University was used. In this analysis, three-dimensional 20 node iso-parametric solid elements, with 8 Gauss points were adopted for the representation of plain and RC elements.

Table 1 Properties of bars

Bar No.	Area (mm^2)	Yield point (MPa)	Elastic modulus
6	31.67	300	165000
10	71.33	360	192000
25	506.7	400	178000

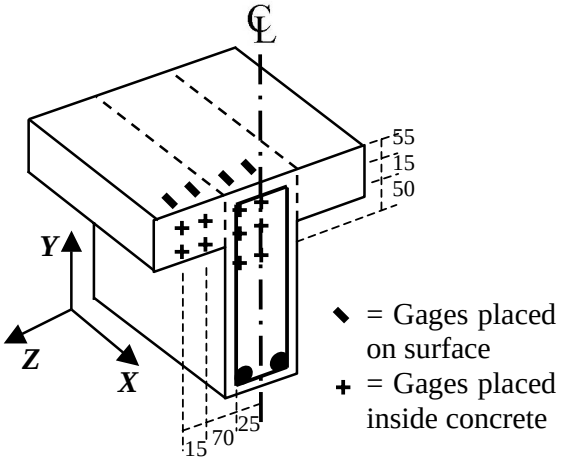

Fig.3 Locations of gages at both sections

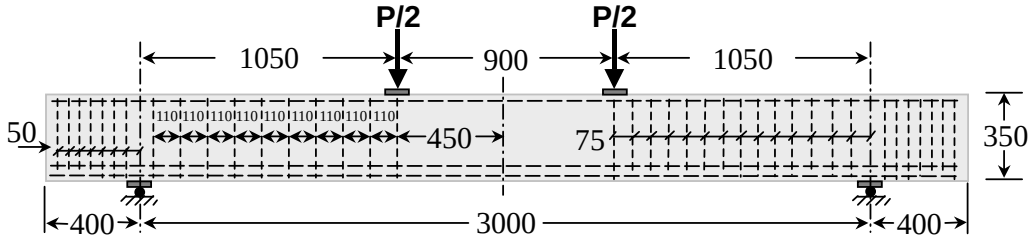

Fig.1 Loading condition and stirrup arrangement (unit: mm)

The nonlinear iterative procedure was controlled by the modified Newton-Raphson method. In this procedure, convergence is judged by the ratio of Σ(Residual force)^2 to Σ(Internal force)^2 and the iteration procedure is repeated until the ratio becomes less than 10^{-6}.

The 3D elasto-plastic fracture model developed by Maekawa et al [2] is used for the concrete model before cracking. In this model, stresses and strains are represented by an equivalent stress and equivalent strain, respectively. The adopted failure criteria that acted in agreement with Niwa's model in tension-compression zone and Aoyanagi and Yamada's model in tension-tension region were extended to three-dimensional criteria by satisfying boundary conditions [3].

The tension-softening model proposed by Reinhardt is adopted for concrete after cracking. The constitutive model for the reinforcing bar in concrete was modeled based both on the properties of bare bars and on the effect of the bond to concrete, at this point, tri-linear model presented by Maekawa et al [3] expressing the strain hardening was adopted. In this analysis, the smeared crack concept and the fixed crack model were adopted and shear transfer stresses were calculated using Li and Maekawa's model [3].

After cracking, the concrete linear softening model for direction parallel to the crack is introduced to consider the effect of cracking on compression-softening. In this model, compressive stress is reduced to zero at limited strain ε_u. The gradient of strain softening is defined by compressive fracture energy consumed in compressive stress parallel to the crack in the tension-compression area. In other words, the softening curve is defined in such a way that the area surrounded by the envelope curve of the stress-strain relation is equal to the fracture energy concept as in tension softening. However, the reduced stress has a limit that is 10% of the compressive strength. In this study, the compression fracture energy used is set to 50 N/mm based on the study of Nakamura et al [4].

4. RESULTS AND DISCUSSION

4.1 Load-Deformation Relationship

Fig.4 shows the comparison of the load-deflection curve for specimens S1 and S2 as reported in the previous work [1].

4.2 Stress Development in Stirrups

A typical pattern of the stress variation in stirrups for increasing loads was measured by the strain gages. The stresses plotted are the average for 3 locations of the stirrups. The location and reference number of stirrups whose strains were measured in the experiment are shown in Fig.5. From Figs.5 and 6, the average stresses of selected stirrups are compared. It can be seen that the average stress of stirrup for both specimens are almost the same at the initial condition. After that, the average stress of stirrup in the T-beam becomes lower than that in the rectangular beam at around 250 kN of the applied load. In experiment, correspondingly, the crack propagated horizontally below the concrete top flange at the same location of the considering stirrups (see Figs.5 and 10 (a)). It can be considered that the lower stress of stirrup in the T-beam is due to the changing in shear resisting mechanism that will be discussed later.

In order to compare tested results with smear-concept FEM results, the averaged stresses between two stirrups are used. Analyzed and measured stirrup stresses at the location between stirrup numbers 3-4 and 6-7 are compared as shown in Fig.7. It is clearly seen that the FEM results can predict the stress development in stirrup and the turning point of the shear mechanism well.

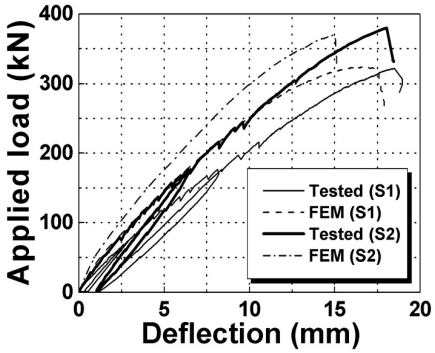

Fig.4 Load-deflection curves

4.3 Stress Distribution on Sections

Shear force (V) can be expressed by two components: arching action and beam action. At any location in a beam when a moment gradient dM/dx is present, these two effects are combined to give the total shear resistance. For a cracked concrete member, these components can be written as follows:

$$V = \frac{dM}{dx} \quad \text{and} \quad M = T \cdot jd \tag{1}$$

Where T and jd are the tensile force in the bottom chord and lever arm, respectively. Thus

$$V = T\frac{djd}{dx} + jd\frac{dT}{dx} \tag{2}$$

The first term of the previous equation refers to the arching action, while the second term describes the beam behavior. These two effects can be evaluated between two known sections along length of beam, thus, Eq. (2) can be rewritten as

$$V = T\frac{\Delta jd}{\Delta x} + jd\frac{\Delta T}{\Delta x} \tag{3}$$

By using the strain gage data in the concrete and bars at sections of stirrup No. 1 and 5 (see Fig.5), the strain distribution on beam sections can be drawn (section of stirrup No. 1, see Fig.8). By indicating the location of the neutral axis at different load step and knowing the applied shear (V), all terms of Eq. (3) are known. Beam action variations for increasing shear force in both specimens were calculated from the experimental results between two sections and shown in Fig.9. Fig.9 shows that shear force starts out being carried entirely by beam action but ends with arching action as predominant for T-beam. The load at which beam and arching actions became different for two specimens is corresponding to the turning point observed from the stress in stirrups. This result also shows the change of the shear mechanism due to the existing of the concrete top flange.

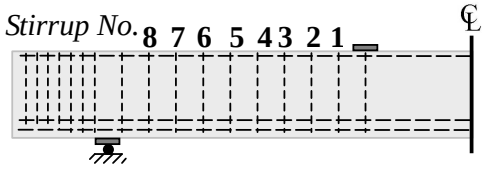

Fig.5 Location and reference number of stirrups whose strains were measured in both specimens

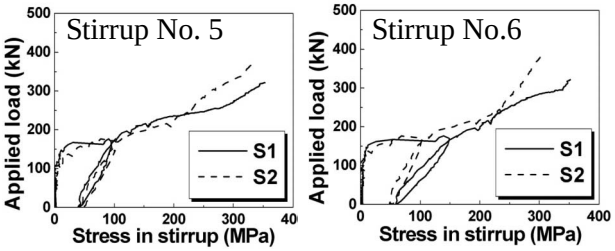

Fig.6 Stress development in stirrups

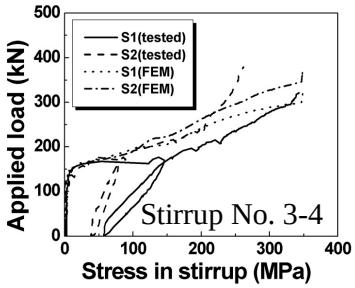

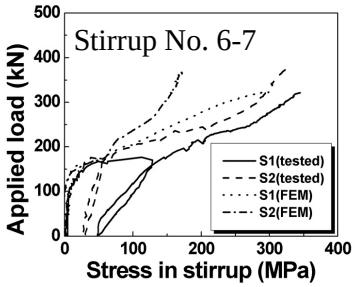

Fig.7 Comparison of analyzed and measured stress development in stirrups

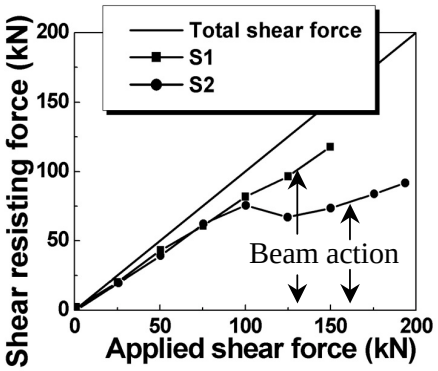

Fig.9 Shear resisting components

4.4 Crack Patterns

Crack pattern of S2 in the experiment were observed as shown in Fig.10 (a). As already mentioned before, the turning point of the shear mechanism observed in the experiment (stirrup stresses and strain distribution on sections) was occurred at the load step when shear crack propagated along the connection zone of the flange and the web. The same observable fact can be observed from the FEM results. Fig.10 (b) show the crack pattern from the FEM before the turning point (lower than 250 kN). It can be seen that the crack angle in the connection zone between the flange and the web are about 45^{o}. Then, the crack with very small crack angle (almost parallel to *X* direction) are observed at the connection zone between the flange and the web at the corresponding load step to the turning point of the shear mechanism (250-300 kN, see Fig.10 (C)). The propagation of the horizontal crack can be confirmed by the sudden increasing of strain in *Y* direction of Gauss's points near the connection zone of the flange and the web at the corresponding load step to the turning point as shown in Fig.10 (C).

5. SHEAR RESISTING MECHANISM

5.1 Governing Mechanism of T-beams

From the experimental results, it can be considered that the shear resisting mechanism of T-beam is almost the same as that of rectangular beam before the appearance of the horizontal crack. At this state, beam behavior is governed by the truss mechanism. After the shear crack propagate horizontally below the concrete top flange, the stirrup stress of T-beam becomes less than that of rectangular beam. It can be considered that it is due to the changing of the governing shear resisting mechanism inside the beam from the truss analogy to the arch mechanism. This is already confirmed by the comparison of shear resisting components (see Fig.9). In the arch mechanism, the concrete area on top flange of T-beam can provide the additional area of the compression zone.

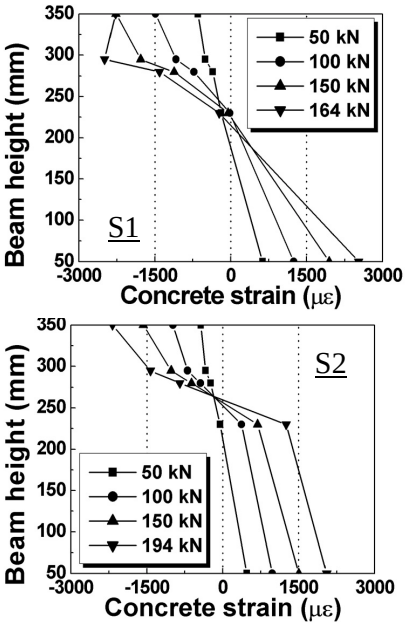

Fig.8 Strain distribution on section 1

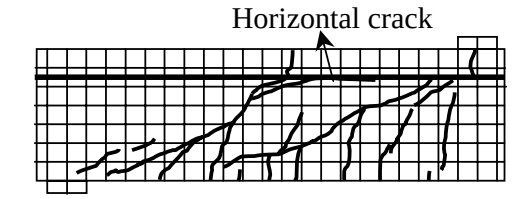

(a) Tested result at failure

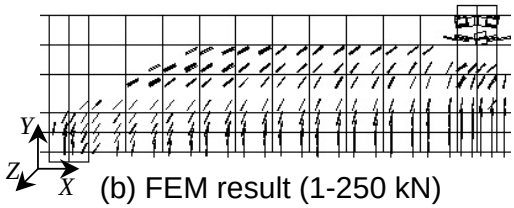

(b) FEM result (1-250 kN)

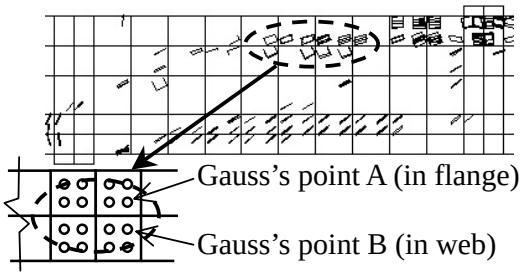

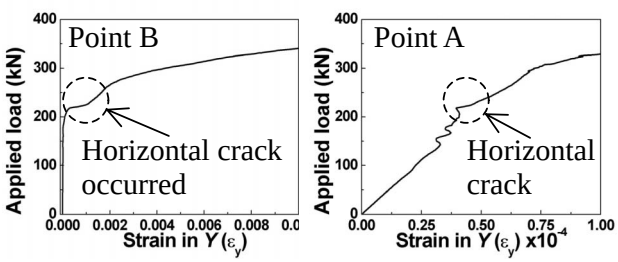

(C) FEM result (250-300 kN) and ε_y

Fig.10 Crack pattern of S2

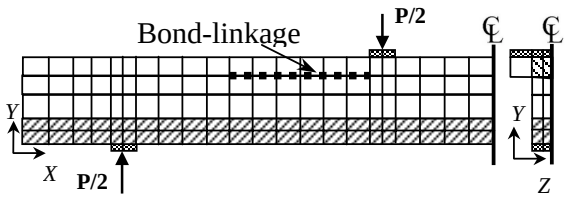

Fig.11 Finite element mesh

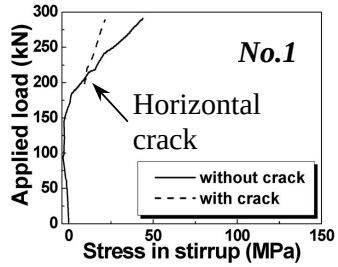

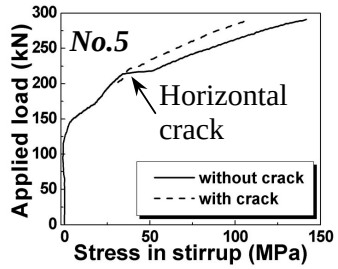

Fig.12 Stress development in stirrups (numerical results)

5.2 Governing Factor for Shear Resisting Mechanism of T-Beams

From the experimental observation, the factor that controls the change of the governing mechanism of T-beam from truss mechanism to arch mechanism is the propagation of the horizontal crack between web and the flange of T-beam. This factor can be verified with the 3D FEM as follow.

Numerical analysis of two specimens, with and without bond-linkage elements, was conducted to simulate the existence of the horizontal crack. Both specimens had the same size as specimen S2.

Bond-linkage element is the layer element containing four Gauss's points. In analysis, bond-linkage elements were installed in the position that the horizontal cracks were observed from the experiment (see Fig.10 (a) and 11). The stiffness of bond-linkage was initially set to the same value of the stiffness of concrete. The horizontal crack was simulated by the sudden reduction of the shear transfer stress of bond-linkage elements at the certain load step after shear crack. The shear transfer stresses were calculated using Li and Maekawa's model [3]. From Fig.12, after the shear transfer stress of bond-linkage elements is reduced (horizontal crack is assumed to be occurred in the analysis), the stress of stirrups in the T-beam with the horizontal crack truly becomes lower than that in the beam without the crack at the same load step. This confirms the influence of the horizontal crack as the governing factor for the shear mechanism of T-beam.

6. CONCLUSIONS

1. Existing of concrete top flange has significant effects on shear resisting mechanism of RC T-beams.
2. The governing shear resisting mechanism of T-beam has been changed from the truss analogy to the arch mechanism as can be observed from the tested results. Also, the turning point can be simulated well by the FEM.
3. The horizontal crack between the flange and the web of T-beam has an influence on the turning point of the shear resisting mechanism.

REFERENCES

[1] Pansuk, W., Sato, Y., Takahashi, R., and Ueda, T., "Influence of Top Flange to Shear Capacity of Reinforced Concrete T-Beams," Proceedings of JCI, Vol. 26, June 2004, pp. 991-996.

[2] Takahashi, R., Sato, Y., Ueda, T., "A simulation of shear failure of steel-concrete composite slab by 3D nonlinear FEM," Journal of Structural Engineering, JSCE, Vol.48A, Mar. 2002. (In Japanese)

[3] Okamura, H., and Maekawa, K., "Nonlinear Analysis and Constitutive Models of Reinforced Concrete," Gihodo-Shuppan Co. Tokyo, 1991.

[4] Nakamura, H., and Higai, T., "Compressive Fracture Energy and Fracture Zone Length of Concrete," Seminar on Post-peak Behavior of RC Structures Subjected to Seismic Loads, 2, 1999, pp. 259-272.